ChemComm

COMMUNICATION

View Article Online
View Journal | View Issue

Cite this: *Chem. Commun.*, 2025, **61**, 14382

Received 30th June 2025,
Accepted 11th August 2025

DOI: 10.1039/d5cc03543k

rsc.li/chemcomm

Guanidinium-linked morpholino-siRNA chimera: synthesis, biophysical properties and *in vitro* activity

Shalini Gupta, † Atanu Ghosh, † Subhamoy Pratihar, Maria Mukherjee, Jayanta Kundu and Surajit Sinha *

This study introduces guanidinium morpholino RNA (GMO-RNA), an RNA analogue with enhanced cell permeability, nuclease resistance and RNA interference activity. Self-penetrating GMO-RNA chimeras leverage guanidinium-mediated endocytic uptake across multiple cell lines. Thermal studies validated duplex stability, and Eg5-targeting GMO-siRNA achieved effective gene silencing in cervical cancer cells, demonstrating therapeutic potential.

Chimeric oligonucleotides have emerged as superior alternatives to conventional oligonucleotide designs, with versatile properties which can be tuned with suitable combinations as per necessity.[1] Though chimeric structures have mainly been associated with single-stranded antisense oligonucleotides,[2] siRNAs may also benefit from the incorporation of short stretches of a suitable modification at positions which do not hinder Argonaute 2 (Ago2, the effector complex for RNA interference) loading and catalytic activity. Apart from lipophilic conjugations such as fatty acids[3] which increase their bioavailability, siRNAs may also be modified with guanidinium groups, which are known for inducing endocytosis.[4] Cationic oligonucleotides, particularly those with guanidinium linkages, exhibit enhanced binding affinity, nuclease resistance, and improved cellular uptake.[5,6] However, possibilities of unfavourable electrostatic interactions of the positively charged guanidinium groups with the negatively charged backbone remain, which may hinder the siRNA activity.[7] On the other hand, incorporation of guanidinium groups as linkages (GMO) in phosphorodiamidate morpholino oligonucleotides (PMOs),[8] with neutral backbones, is known to facilitate their uptake and enhance antisense activity while modulating the net charge and global conformation.[9,10] As linkages between a 5′ primary amine and 3′-secondary amines of morpholinos, guanidinium groups have lower flexibility than deoxyribonucleic guanidines (DNGs),[11] with reduced possibility for intra/inter-strand interactions.

School of Applied and Interdisciplinary Sciences, Indian Association for the Cultivation of Science, Jadavpur, Kolkata 700032, India. E-mail: ocss5@iacs.res.in
† These authors contributed equally to this work.

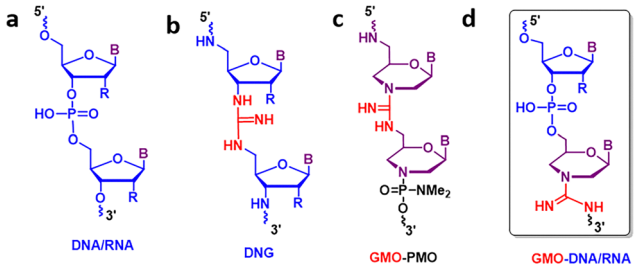

Fig. 1 General structure of (a) DNA/RNA, (b) DNG, (c) GMO-PMO and (d) GMO-DNA/RNA.

In this study, we report GMO-DNA and GMO-RNA chimeras with four GMO units incorporated at the 3′-end in the conventional 3′ to 5′ direction (Fig. 1). By introducing the GMO moiety, we aimed to enhance the cellular permeability and nuclease resistance of the modified oligonucleotides while maintaining the catalytic activity (Ago2 loading) when incorporated in the antisense strand of an siRNA.

For synthesis of GMO, morpholino monomers were synthesized from ribonucleoside (**1**) using standard protection and deprotection chemistry (Fig. 2 and Schemes S1, S2, SI). To adapt the protocol for automated DNA/RNA synthesis, the GMO stretch was incorporated at the 3′ end by manual coupling steps, utilizing morpholino monomers (**2**, **3** and **4**) with a 5′-amino terminal. The at-a-stretch synthesis began by attaching an Fmoc-protected linker **5** to LCAA CPG resin followed by Fmoc deprotection and coupling of monomer **3** using $HgCl_2$ and *N*-ethyl morpholine (NEM) in NMP as the solvent.[10] However, trityl assays showed low coupling efficiency, likely due to

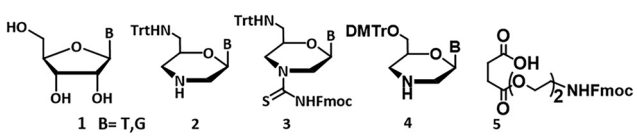

Fig. 2 Structure of the morpholino monomers and linker used in chimera synthesis.

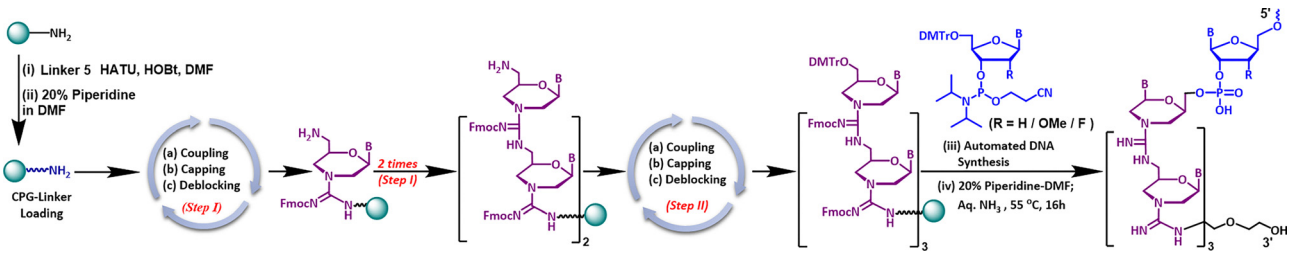

Scheme 1 Solid-phase synthesis of GMO-DNA and GMO-RNA chimera. Reagents and conditions: step I (a) coupling: (i) FmocNCS (5 equiv.) in dry DCM (3 times 30 min = 90 min), (ii) 5′-NHTrt protected morpholino monomer **2** (5 equiv.), $HgCl_2$ (5 equiv.), NEM (5 equiv.), NMP, (3 times 2 h = 6 h); in step II coupling was done by 5′-DMTr protected morpholino monomer **4**. (b) Capping: (1 : 1) 20% Ac_2O in NMP and 20% DIPEA in NMP (3 times 1 min = 3 min); (c) deblocking: CYPTFA (3-cyano pyridine, TFA, CF_3COOH, DCM) (for Tr) or 3% TCA in DCM (for DMTr), (5 times 2 min = 10 min).

the morpholino ring nitrogen interfering with carbodiimide intermediate formation. To address this, an alternative approach was implemented where FmocNCS reagent was added to the solid support before coupling monomer **2** under the same conditions, improving the yield to 93% (Scheme 1).

This procedure was repeated to incorporate three GMO units, followed by coupling with 5′OH containing monomer **4**, to enable the continuation of DNA and RNA synthesis *via* standard phosphoramidite chemistry to obtain GMO-DNA and GMO-RNA chimeras (Scheme 1 and Scheme S3, SI). 2′-Substituted (OMe and F) amidites were used for the latter. In this way, a total of four guanidinium groups were incorporated in line with our previous study of IGT conjugated siRNA.[12] The oligonucleotides were cleaved using standard conditions, purified by HPLC (Fig. S1–S6, SI), and characterized using MALDI-TOF (Fig. S7–S10, SI). The synthesized oligo sequence and HPLC yield are summarized in Tables S1 and S2, SI. Unfortunately, the GMO part was fragmented during MALDI analysis (Fig. S8b, SI). The biophysical properties (thermal melting and circular dichroism) of the synthesized chimeric oligonucleotides were analysed and compared to their unmodified DNA and RNA. For this, a model 14-mer sequence was chosen for comparison in DNA (**ON1** *vs.* **ON2**), 2′-OMe substituted RNA (**ON3** *vs.* **ON4**) and alternatively substituted 2′-OMe/2′-F RNA (**ON5** *vs.* **ON6**) backbones with complementary strands (both DNA and 2′-OH RNA). The latter is frequently used in therapeutic siRNAs for improved stability and RISC loading. The results revealed that the GMO incorporation in all backbones destabilized the duplex in comparison with the unmodified oligonucleotides, with the effect being more pronounced with complementary RNA. However, the destabilization in the 2′-OMe/2′-F RNA backbone (common for siRNAs) was lower than that in the 2′-OMe RNA backbone (common for antisense oligonucleotides). Interestingly, GMO incorporation partly in the overhang of a full-length siRNA duplex (**cMyc R-OF** *vs.* **GR-OF**) did not affect the Watson Crick base pairing but the T_m decreased for GMO analogues (Table 1 and Fig. S11–S18, SI). In circular dichroism study, the duplex formed by the 14-mer oligonucleotides with complementary DNA and RNA showed characteristic positive peaks at approximately ~265 nm and ~212 nm and a negative band at ~245 nm except for the the regular DNA, which indicated a B type helical structure, while GMO-siRNAs adopt similar global geometry as unmodified partners (Fig. S19, SI).

Table 1 Sequences of oligonucleotides used in the study and their thermal melting analysis with complementary DNA/RNA

Entry		Sequences (3′ → 5′)	T_m (°C) DNA	ΔT_m (°C)	T_m (°C) RNA	ΔT_m (°C)
ON1		**ttttgtctttacag**	40	3	40	3.5
ON2		**TTTTgtctttacag**	37		36.5	
ON3		**UUUUGTCUUUACAG**	30.5	n.t.	53	12.5
ON4		**TTTTGTCUUUACAG**	n.t.		40.5	
ON5		**UUUUGUCUUUACAG**	33	8	56	9.5
ON6		**TTTTGUCUUUACAG**	25		46.5	
siRNA	cMyc R- OF	5'-AACAGAAAUGUCCUGAGCAAUtt-3' / 3'-ttUUGUCUUUACAGGACUCGUUA-5'			84	1
	cMyc GR- OF	5'-AACAGAAAUGUCCUGAGCAAUtt-3' / 3'-TTTTGUCUUUACAGGACUCGUUA-5'			83	
	Eg5 R- OF	5'- CAACAAGGAUGAAGUCUAU-3' / 3'- GUUGUUCCUACUUCAGAUA -5'			73	12
	Eg5 GR- OF	5'-CAACAAGGAUGAAGUCUAU-3' / 3'- GTTGUUCCUACUUCAGAUA -5'			61	

Conditions: 40 mM phosphate buffer (pH 7)/100 mM NaCl, with concentration of 2 μM (each strand). T_m values reported are the averages of two independent experiments that are within ±1.0 °C. ΔT_m values are calculated w.r.t. melting temperatures of the corresponding analogue with no GMO modification; n.t.: no clear transition observed; red represents the guanidinium morpholino oligonucleotide (GMO) part, blue for 2′-OMe, green for 2′-F monomers, and lowercase indicates 2-deoxy monomers.

The stability of oligonucleotides towards serum nucleases is critical for the development of therapeutic oligonucleotides. These studies were performed on the model 14-mer sequences in the presence of 10% FBS (fetal bovine serum) or 3′-exonuclease. Remarkably, the modified oligonucleotides exhibited greater stability compared to their unmodified counterparts, with significant improvement in DNA and 2′-OMe/F RNA backbones (Fig. 3 and Fig. S20, SI). The resistance to enzymatic digestion can be attributed to the presence of the unnatural rigid guanidinium linkage in the GMO moiety. In line with our objective, the cellular internalization properties of a 23-mer GMO-modified oligonucleotide (GR-2′-OMe, ON8, see SI for sequence) with FAM conjugation was studied in multiple

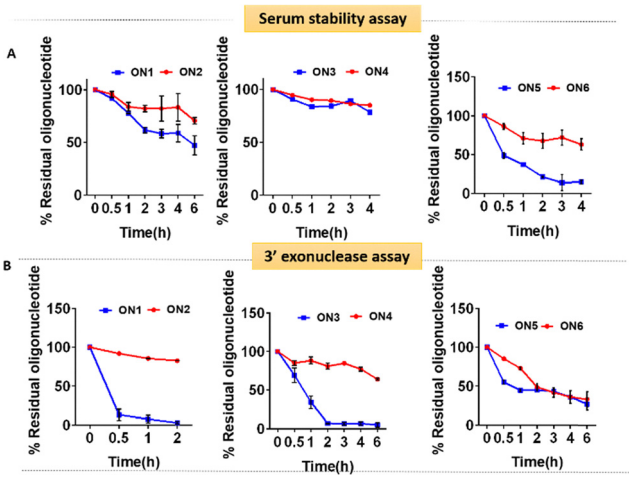

Fig. 3 Stability of oligonucleotides in (A) serum and (B) 3′ exonuclease in comparison to their unmodified counterparts represented in blue.

cancer cell lines (prostate cancer: PC-3 and DU 145; breast cancer: MDA-MB-231 and MCF7; liver cancer: HepG2) alongside the FAM conjugated unmodified oligonucleotide (R-2′-OMe, ON7). A full 2′-OMe backbone (single strand as well as duplex) was selected for this study because of its excellent stability, which would enable a more accurate interpretation of uptake/localization in the cells. Both single strand uptake and duplex uptake were quantified (Fig. 4A). The single strand uptake was variable across the studied cell lines, with greater selectivity in the PC-3 and MCF7 cell lines over the unmodified oligonucleotide. The internalisation of the duplex was then investigated in these two cell lines with variation in serum composition. It was found that the GMO duplex uptake was more efficient in optimum serum conditions (10%) and this effect was more enhanced in MCF7 cells. Furthermore, with MCF7 as the chosen cell line, the intracellular localization of the FAM duplexes was determined by confocal microscopy in live cells (Fig. 4B) where it was found that the GR-2′-OMe duplex showed greater accumulation, albeit having partial colocalization with the late

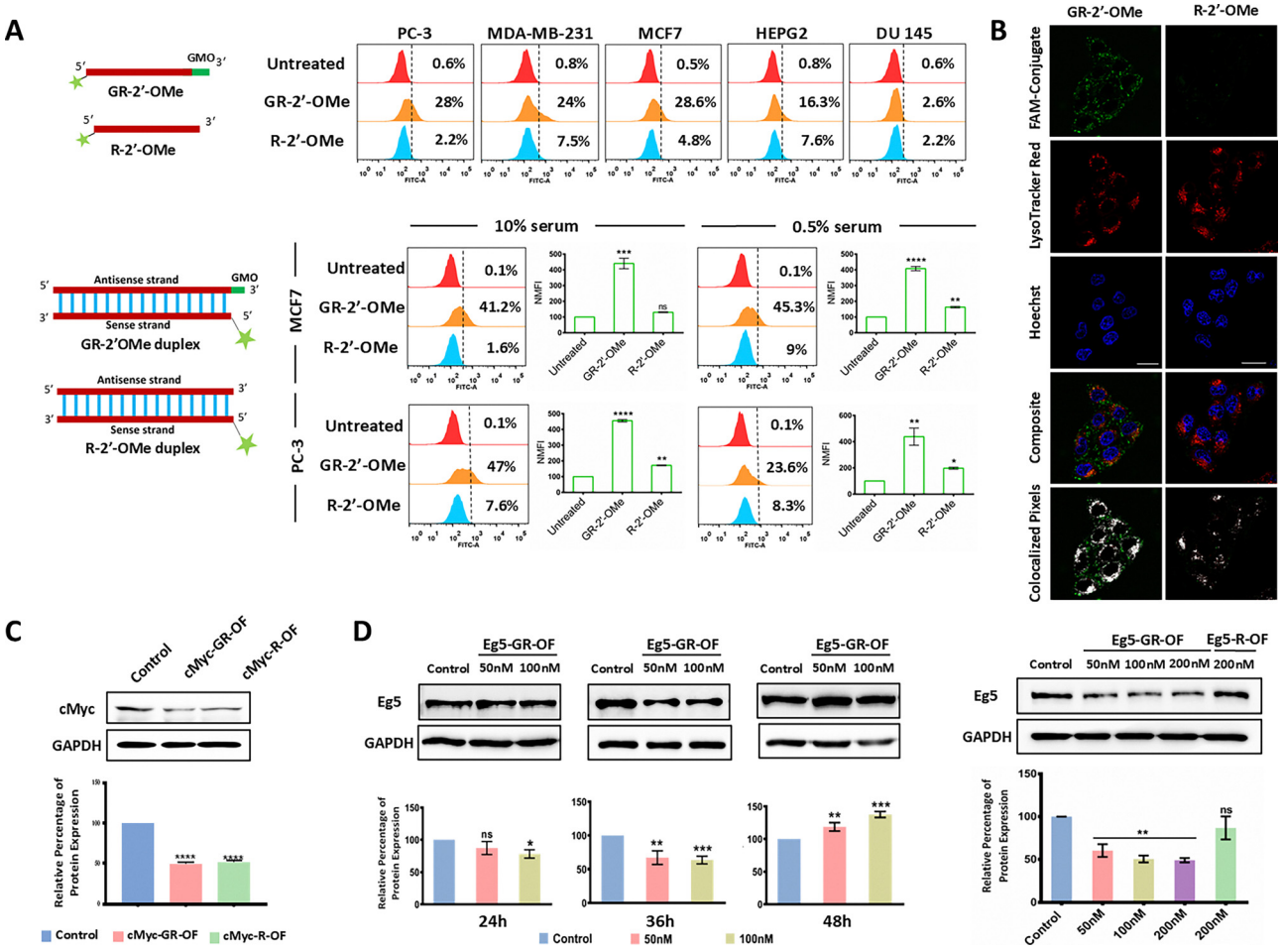

Fig. 4 (A) Cellular internalization studies of single strand and duplex GMO modified 2′-OMe strands in multiple cell lines after 5 h of incubation. Histogram plots and respective bar diagrams depict percentage uptake in comparison to untreated controls. Data presented as mean ± SEM. *$p < 0.05$. (B) Confocal images for FAM-conjugated duplexes in live MCF7 cells after 5 h in 10% serum. Scale bar 20 μm. (C) Western blot (WB) analysis for RISC validation using cMyc siRNA (250 nM) with Lipofectamine. (D) WB analysis of Eg5 down regulation in HeLa cells at varying time points and doses in comparison with an unmodified duplex. Data presented as mean ± SEM. *$p < 0.05$.

endosomal/lysosomal marker LysoTracker Red (Pearson's coefficient: 0.62 for GR-2′-OMe and 0.95 for R-2′-OMe). Overall, these findings demonstrated the role of the guanidinium linkage in facilitating cellular uptake and suggested that the GMO modification could hold promise for enhancing the delivery and intracellular localization of oligonucleotides for potential therapeutic applications.

Lower duplex destabilization due to GMO incorporation in the 2′-OMe/2′-F backbone prompted us to study its biological effect in a model siRNA to determine whether this modification could hamper the formation of the RNA induced silencing complex (RISC) by compromising Ago2 loading. The 3′-end of the antisense strand was chosen for GMO incorporation as it has minimal effect on Ago2 loading[4,13] and a model siRNA sequence against cMyc, a proto-oncogenic factor overexpressed in cancer cells,[14] was chosen for studying its activity in MCF-7 cells. Though the sequence was validated with a 2′-OH backbone,[15] we adapted it to an alternating 2′-OMe/2′-F backbone, which is more stable and mimics therapeutic oligonucleotides more closely.[16] For RISC validation, both duplexes were transfected with Lipofectamine 3000 and the target suppression was observed by western blotting. Almost ∼50% knockdown was observed at a 250 nM dose for both duplexes to a similar extent, which signified that GMO incorporation did not hinder the silencing ability of the duplex siRNA (Fig. 4C). cMyc related markers such as N-Cad,[17] E-Cad[18] and lactate dehydrogenase-A (LDHA)[19] also exhibited the expected expression profiles in response to c-Myc downregulation, confirming the efficacy of the modified siRNA (Fig. S21A, SI). However, optimum silencing could not be achieved at a lower dose (100 nM) with Lipofectamine (Fig. S21B, SI). Moreover, no silencing activity of the siRNA was observed on gymnotic uptake at different time points (Fig. S21C, SI), up to the dose of 500 nM (Fig. S21D, SI) in MCF7 cells. This signified that the siRNA was not very active, and probably the adaptation of the 2′-modifications hindered its silencing ability.

To evaluate the effect of GMO modification on gymnotic uptake, an established and potent siRNA sequence was chosen, which targeted Eg5, also known as kinesin like protein KIF11, in HeLa cells.[20] The Eg5 GMO-siRNA duplex treatment was performed in optimum serum at 50 nM & 100 nM doses at 24, 36, and 48-hour time points and untreated cells served as positive controls (Fig. 4D). Transient knockdown was observed at both doses, with maximal inhibition at 36 hours. Dose-dependent inhibition studies at 36 h were further conducted using 50 nM, 100 nM, and 200 nM GMO-siRNA against Eg5 and the unmodified siRNA at the highest dose (200 nM) served as the negative control. Eg5 protein expression was significantly down regulated at 50 nM of the **Eg5-GR-OF** treatment but the effect somewhat plateaued even on increasing the dose,[21,22] which could be due to endosomal block. The negative control did not show significant suppression even at the highest dose.

In conclusion, this study highlights the development of novel GMO-DNA and RNA chimeras with improved nuclease and serum stability. GMO incorporation in the 2′-OMe RNA backbone enhanced its cellular uptake, whereas the Ago2 loading efficiency was unhindered in the 2′-OMe/2′-F RNA backbone. Notably, GMO incorporation showed efficient gymnotic uptake with significant target knockdown in an established Eg5 siRNA at low doses. These findings underscore the potential of GMO as a promising modification for creating stable, effective therapeutic siRNA molecules with improved delivery.

S. S. thanks SERB SUPRA SPR/2023/000358 for the financial support.

Conflicts of interest

There are no conflicts to declare.

Data availability

The data supporting this article have been included as part of the SI. Experimental procedure, compound characterization data, biological experiment figure and raw image of western blot and electrophoresis data. See DOI: **https://doi.org/10.1039/d5cc03543k**

Notes and references

1 M. Egli and M. Manoharan, *Nucleic Acids Res.*, 2023, **51**, 2529–2573.
2 T. C. Roberts, R. Langer and M. J. A. Wood, *Nat. Rev. Drug Discovery*, 2020, **19**, 673–694.
3 T. Kubo, K. Yanagihara, Y. Takei, K. Mihara, Y. Morita and T. Seyama, *Mol. Pharm.*, 2011, **8**, 2193–2203.
4 G. N. Nawale, S. Bahadorikhalili, P. Sengupta, S. Kadekar, S. Chatterjee and O. P. Varghese, *Chem. Commun.*, 2019, **55**, 9112–9115.
5 G. Deglane, S. Abes, T. Michel, P. Prevot, E. Vivès, F. Debart, I. Barvík, B. Lebleu and J.-J. Vasseur, *Chem. Biochem.*, 2006, **7**, 684–692.
6 A. R. Shrestha, Y. Kotobuki, Y. Hari and S. Obika, *Chem. Commun.*, 2014, **50**, 575–577; T. Yamaguchi, N. Horie, H. Aoyama, S. Kumagai and S. Obika, *Nucleic Acids Res.*, 2023, **51**, 7749–7761.
7 M. Gooding, L. P. Browne, F. M. Quinteiro and D. L. Selwood, *Chem. Biol. Drug Des.*, 2012, **80**, 787–809.
8 A. Ghosh, A. Banerjee, S. Gupta and S. Sinha, *J. Am. Chem. Soc.*, 2024, **146**, 32989–33001.
9 K. Tarbashevich, A. Ghosh, A. Das, D. Kuilya, S. N. Sharma, S. Sinha and E. Raz, *Nat. Commun.*, 2025, **16**, 3614.
10 U. Das, J. Kundu, P. Shaw, C. Bose, A. Ghosh, S. Gupta, S. Sarkar, J. Bhadra and S. Sinha, *Mol. Ther. Nucleic Acids*, 2023, **32**, 203–228.
11 B. A. Linkletter, I. E. Szabo and T. C. Bruice, *J. Am. Chem. Soc.*, 1999, **121**, 3888–3896.
12 S. Gupta, U. Das and S. Sinha, *Bioorg. Med. Chem. Lett.*, 2022, **76**, 129017.
13 A. J. Varley and J. P. Desaulniers, *RSC Adv.*, 2021, **11**, 2415–2426.
14 D. M. Miller, S. D. Thomas, A. Islam, D. Muench and K. Sedoris, *Clin. Cancer Res.*, 2012, **18**, 5546–5553.
15 Y. Zhang, L. Peng, R. J. Mumper and L. Huang, *Biomaterials*, 2013, **34**, 8459–8468.
16 B. Hu, L. Zhong, Y. Weng, L. Peng, Y. Huang, Y. Zhao and X. J. Liang, *Signal Transduction Targeted Ther.*, 2020, **5**, 101.
17 C. Y. Loh, J. Y. Chai, T. F. Tang, W. F. Wong, G. Sethi, M. K. Shanmugam, P. P. Chong and C. Y. Looi, *Cells*, 2019, **8**, 1118.
18 V. H. Cowling and M. D. Cole, *Oncogene*, 2007, **26**, 3582–3586.
19 B. C. Lewis, J. E. Prescott, S. E. Campbell, H. Shim, R. Z. Orlowski and C. V. Dang, *Cancer Res.*, 2000, **60**, 6178–6183.
20 E. Koller, S. Propp, H. Murray, W. Lima, B. Bhat, T. P. Prakash, C. R. Allerson, E. E. Swayze, E. G. Marcusson and N. M. Dean, *Nucleic Acids Res.*, 2006, **34**, 4467–4476.
21 T. O. Kabilova, E. L. Chernolovskaya, A. V. Vladimirova and V. V. Vlassov, *Oligonucleotides*, 2006, **16**, 15–25.
22 A. Kalota, L. Karabon, C. R. Swider, E. Viazovkina, M. Elzagheid, M. J. Damha and A. M. Gewirtz, *Nucleic Acids Res.*, 2006, **34**, 451–461.